Perurbation theory

One way to go beyond the static mean field approximation is to explore the higher order terms in perturbation theory with respect to Coulomb interaction.

This is not an optimal way of improving precision of the approximation, as we will show below. But is the most direct non-static approach, and when combined with more modern approaches, such as the Dynamical Mean Field Theory, can lead to even qualitatively correct physics in some important models.

The first order approximation in U is the Hartree-Fock approximation. Although quite succesful for atoms and small molecules, it fails very badly in solids.

The Hartree term is just the classical electrostatic term:

$$E_H[\rho] = \frac{1}{2}\int d^3r \int d^3r' \rho(\mathbf{r})\rho(\mathbf{r}')V_C(\mathbf{r}-\mathbf{r}') \tag{1}$$

The Fock term, required by the Pauli exclusion principle, has already quantum mechanical

origin, but is still static:

$$E_X[\rho] = -\frac{1}{2}\sum_{\sigma}\int d^3r \int d^3r' \rho_\sigma(\mathbf{r},\mathbf{r}')\rho_\sigma(\mathbf{r}',\mathbf{r})V_C(\mathbf{r}-\mathbf{r}') \quad (2)$$

The generalization of the exchange Feynman graph is so called GW (when the interaction becomes dressed), an approximation that gained popularity in recent years, because it became feasible to use it for realistic systems.

In simple models like Hubbard model, the static terms are just absorbed in the chemical potential.

The next order correction is the second order term in the interaction. In this exercise, we will code the second order perturbation theory for the one band lattice model. We will then realize that the self-energy is roughly momentum independent, hence we will concentrate on the local approximation.

In the case of a purely local self-energy, the dynamical mean field theory allows one to compute such local self-energy exactly by solving an auxiliary (quantum impurity) problem.

It turns out that if we use the second order perturbation theory to solve the auxiliary (quantum impurity) system, rather than the original system, the same second order

approximation leads to better results. It captures on qualitative level the Mott transition, which direct second order perturbation theory does not. The approximation in this context is called the Iterative Perturbation Theory (IPT). We will code the IPT algorithm and compare its performance to straighforward perturbation theory.

1 The second order perturbation theory

1.1 Derivation of the second order term

Lets consider the simplest one band model, the Hubbard model

$$H = \sum_{\mathbf{k}} \epsilon_{\mathbf{k}} c^{\dagger}_{\mathbf{k}\sigma} c_{\mathbf{k}\sigma} + \sum_{i} U n_{i\uparrow} n_{i\downarrow} \tag{3}$$

The first order Hartree-Fock self-energy is

$$\Sigma_{\sigma} = U n_{\bar{\sigma}}.$$

In paramagnetic state, this is just a constant $Un/2$ and it will lead to a shift in the chemical potential.

The second order term is

$$\Sigma_{\mathbf{k}}(i\omega) = -\frac{U^2}{\beta^2} \sum_{i\omega',\mathbf{k}',\mathbf{q},i\Omega} G_{\mathbf{k}'}(i\omega')G_{\mathbf{k}'-\mathbf{q}}(i\omega'-i\Omega)G_{\mathbf{k}-\mathbf{q}}(i\omega-i\Omega) \tag{4}$$

(exercise for the reader: Please draw the Feynman diagram and mark the propagators with frequency and momentum compatible with the equation.)

Alternatively, we can introduce the polarizability bubble

$$P_{\mathbf{q}}(i\Omega) = \frac{1}{\beta} \sum_{i\omega',\mathbf{k}'} G_{\mathbf{k}'}(i\omega')G_{\mathbf{k}'-\mathbf{q}}(i\omega'-i\Omega) \tag{5}$$

and the self-energy then has the Fock form

$$\Sigma_{\mathbf{k}}(i\omega) = -\frac{U^2}{\beta} \sum_{\mathbf{q},i\Omega} G_{\mathbf{k}-\mathbf{q}}(i\omega-i\Omega)P_{\mathbf{q}}(i\Omega) \tag{6}$$

The imaginary axis equations can be continued to the real axis. We carry out the standard contour integration

$$P_{\mathbf{q}}(i\Omega) = -\oint \frac{dz}{2\pi i} f(z)G_{\mathbf{k}'}(z)G_{\mathbf{k}'-\mathbf{q}}(z-i\Omega) \tag{7}$$

where contour avoids the branch cuts on the real axis $Imz = 0$ and at $Imz = i\Omega$.

We thus obtain

$$P_{\mathbf{q}}(\Omega) = -\sum_{\mathbf{k}'} \int \frac{dx}{\pi} \left[f(x) G''_{\mathbf{k}'}(x) G^*_{\mathbf{k}'-\mathbf{q}}(x-\Omega) + f(x) G_{\mathbf{k}'}(x+\Omega) G''_{\mathbf{k}'-\mathbf{q}}(x) \right] \tag{8}$$

The self-energy can be contined to the real axis with the same technique, to obtain

$$\Sigma_{\mathbf{k}}(\omega) = -U^2 \int \frac{dx}{\pi} [n(x) P''_{\mathbf{q}}(x) G_{\mathbf{k}-\mathbf{q}}(\omega - x) + f(x) P_{\mathbf{q}}(\omega + x) G''_{\mathbf{k}-\mathbf{q}}(-x)] \tag{9}$$

We did not yet specify what is G in these equations. In the so-called bare perturbation theory $G(\omega) = 1/(\omega - \epsilon_{\mathbf{k}} + i\delta)$ is the non-interacting Green's function (sometimes also denoted by G^0).

Using the well known relation

$$\frac{1}{\omega - \epsilon_{\mathbf{k}} + i\delta} = -i\pi\delta(\omega - \epsilon_{\mathbf{k}}) + \mathcal{P}\frac{1}{\omega - \epsilon_{\mathbf{k}}}$$

we obtain the following simplification

$$P_{\mathbf{q}}(\Omega) = \sum_{\mathbf{k}'} \frac{f(\epsilon_{\mathbf{k}'-\mathbf{q}}) - f(\epsilon_{\mathbf{k}'})}{\Omega - \epsilon_{\mathbf{k}'} + \epsilon_{\mathbf{k}'-\mathbf{q}} + i\delta}. \tag{10}$$

Inserting P into Σ, we can simplify Σ to

$$\Sigma_{\mathbf{k}}(\omega) = U^2 \sum_{\mathbf{k}'\mathbf{q}} n(\epsilon_{\mathbf{k}'} - \epsilon_{\mathbf{k}'-\mathbf{q}}) G_{\mathbf{k}-\mathbf{q}}(\omega - \epsilon_{\mathbf{k}'} + \epsilon_{\mathbf{k}'-\mathbf{q}})[f(\epsilon_{\mathbf{k}'-\mathbf{q}}) - f(\epsilon_{\mathbf{k}'})]$$
$$+U^2 \sum_{\mathbf{q}} f(-\epsilon_{\mathbf{k}-\mathbf{q}}) P_{\mathbf{q}}(\omega - \epsilon_{\mathbf{k}-\mathbf{q}}) \tag{11}$$

which can be brought to the form

$$\Sigma_{\mathbf{k}}(\omega) = U^2 \sum_{\mathbf{k}',\mathbf{q}} \frac{[n(\epsilon_{\mathbf{k}'} - \epsilon_{\mathbf{k}'-\mathbf{q}}) + f(-\epsilon_{\mathbf{k}-\mathbf{q}})][f(\epsilon_{\mathbf{k}'-\mathbf{q}}) - f(\epsilon_{\mathbf{k}'})]}{\omega - \epsilon_{\mathbf{k}'} + \epsilon_{\mathbf{k}'-\mathbf{q}} - \epsilon_{\mathbf{k}-\mathbf{q}} + i\delta} \tag{12}$$

The fermi and bose functions can be rewritten into more simetric way. Let's denote $x = \epsilon_{\mathbf{k}'}$, $y = \epsilon_{\mathbf{k}'-\mathbf{q}}$ and $z = \epsilon_{\mathbf{k}-\mathbf{q}}$.

We have the combination

$$[n(x-y) + f(-z)][f(y) - f(x)] = \tag{13}$$

$$= \frac{1}{(e^x+1)(e^{-y}+1)} + \frac{e^{x-y}-1}{(e^{-z}+1)(e^x+1)(e^{-y}+1)} \tag{14}$$

$$= \frac{1}{(1+e^z)(1+e^x)(1+e^{-y})} + \frac{1}{(1+e^{-z})(1+e^{-x})(1+e^y)} \tag{15}$$

$$f(z)f(x)f(-y) + f(-z)f(-x)f(y) \tag{16}$$

Hence the result is

$$\Sigma_{\mathbf{k}}(\omega) = U^2 \sum_{\mathbf{k}',\mathbf{q}} \frac{f(\epsilon_{\mathbf{k}-\mathbf{q}})f(\epsilon_{\mathbf{k}'})f(-\epsilon_{\mathbf{k}'-\mathbf{q}}) + f(-\epsilon_{\mathbf{k}-\mathbf{q}})f(-\epsilon_{\mathbf{k}'})f(\epsilon_{\mathbf{k}'-\mathbf{q}})}{\omega - \epsilon_{\mathbf{k}'} + \epsilon_{\mathbf{k}'-\mathbf{q}} - \epsilon_{\mathbf{k}-\mathbf{q}} + i\delta} \tag{17}$$

The computation of this self-energy requires 3 nested momentum loops and one frequency loop (one momentum loop over $\mathbf{k}$, and two over $\mathbf{k}'$, $\mathbf{q}$). This can be very slow when large number of momentum points is needed. It is preferable to have one frequency loop and two momenum loop. This is achieved by defining the appropriate polarization bubbles

$$P^{(1)}_{\mathbf{q}}(\Omega) = \sum_{\mathbf{k}'} \frac{f(-\epsilon_{\mathbf{k}'})f(\epsilon_{\mathbf{k}'-\mathbf{q}})}{\Omega - \epsilon_{\mathbf{k}'} + \epsilon_{\mathbf{k}'-\mathbf{q}} + i\delta} \tag{18}$$

$$P^{(2)}_{\mathbf{q}}(\Omega) = \sum_{\mathbf{k}'} \frac{f(\epsilon_{\mathbf{k}'})f(-\epsilon_{\mathbf{k}'-\mathbf{q}})}{\Omega - \epsilon_{\mathbf{k}'} + \epsilon_{\mathbf{k}'-\mathbf{q}} + i\delta} \tag{19}$$

and the self-energy in terms of the polarization

$$\Sigma_{\mathbf{k}}(\omega) = U^2 \sum_{\mathbf{q}} f(-\epsilon_{\mathbf{k}-\mathbf{q}}) P^{(1)}_{\mathbf{q}}(\omega - \epsilon_{\mathbf{k}-\mathbf{q}}) + f(\epsilon_{\mathbf{k}-\mathbf{q}}) P^{(2)}_{\mathbf{q}}(\omega - \epsilon_{\mathbf{k}-\mathbf{q}}) \quad (20)$$

All three equations for $P^{(1)}$, $P^{(2)}$ and $\Sigma_{\mathbf{k}}$ require only one frequency and two momentum nested loops. Furthermore, all terms in the sum are causal (all imaginary parts are negative), hence this expression leads to very stable numerical evaluation.

We will code the Eqns. (18), (19) and (20). Once the self-energy $\Sigma_{\mathbf{k}}(\omega)$ is computed, we will recompute the Green's function by the Dyson equation

$$G_{\mathbf{k}}(\omega) = \frac{1}{\omega - \epsilon_{\mathbf{k}} - \Sigma_{\mathbf{k}}(\omega)}. \quad (21)$$

And finallly, we will print the local Green's function

$$G_{loc}(\omega) = \sum_{\mathbf{k}} G_{\mathbf{k}}(\omega). \quad (22)$$

1.2 Algorithm:

- Generate a regular frequency mesh in the interval [-4,4] with unit of energy $t = 1/4$ in 2D, and $t = 1/(4\sqrt{3})$ for fcc lattice. The order of 200 points should suffice.
- Generate a regular 2D (3D) momentum mesh of k-points. We could use the irreducible part of the 1-st Brillouin zone only, but it is simpler to use the entire 1-st Brillouin zone $\mathbf{k} = \vec{b}_1 x_1 + \vec{b}_2 x_2 + \vec{b}_3 x_3$ and $x_i \in [0, 1)$. Make a list of all points.
- On this momentum mesh, compute the following quantities:
  - dispersion: $\epsilon_{\mathbf{k}}$
    - In 2D n.n. hopping we have $\epsilon_{\mathbf{k}} = -2t(\cos k_x + \cos k_y)$
    - In 3D fcc lattice and n.n. hopping we have

$$\vec{b}_1 = 2\pi(1, 1, -1) \qquad \vec{b}_2 = 2\pi(1, -1, 1) \qquad \vec{b}_3 = 2\pi(-1, 1, 1) \tag{23}$$

$$\mathbf{k} = \vec{b}_1 k_1 + \vec{b}_2 k_2 + \vec{b}_3 k_3 \tag{24}$$

$$\epsilon_{\mathbf{k}} = -4t(\cos\frac{k_x}{2}\cos\frac{k_y}{2} + \cos\frac{k_x}{2}\cos\frac{k_z}{2} + \cos\frac{k_y}{2}\cos\frac{k_z}{2}) \tag{25}$$

  - fermi function: $f(\epsilon_{\mathbf{k}})$

– an index table for: $\mathbf{k}-\mathbf{q}$. For a given index of $\mathbf{k}$ and $\mathbf{q}$ points (ik and iq), the table should give index for vector $\mathbf{k}-\mathbf{q}$: $ikq = ik\_m\_iq[ik, iq]$. Be careful to translate any momentum point back to the 1-st Brillouin zone. To create this table, you will likely need to write the code in some other faster programing language, either fortran and use f2py, or C++ and use weave.

In 3D fcc case you should calculate the projection of $\mathbf{k}-\mathbf{q}$ onto $\vec{b}_i$ i.e., $(\mathbf{k}-\mathbf{q})\cdot a_i/(2\pi) \equiv x_i$, and then make sure that the projection x_i is between 0 and 1. You will need the direct vectors of the fcc lattice

$$a_1 = \frac{1}{2}(1,1,0) \qquad a_2 = \frac{1}{2}(1,0,1) \qquad a_3 = \frac{1}{2}(0,1,1) \tag{26}$$

- Compute the polarization $P^{(1)}$ and $P^{(2)}$ on your frequency and momentum mesh (Eqs. 18 and 19). You will need one loop over frequency and two loops over momentum. Optimization with C++ or fortran is necessary.
- Compute self-energy Eq. 20 on the same mesh. You will need to interpolate the polarization at some arbitrary frequency point ($\omega - \epsilon_{\mathbf{k}-\mathbf{q}}$). You can use linear interpolation.
- Finally compute the Green's function G_{loc} of Eq. 22. Again we have one frequency and

two momentum loops. Optimization is necessary.

- Plot the Density of States $D(\omega) = -\frac{1}{\pi} ImG_{loc}(\omega)$.

1.3 Results

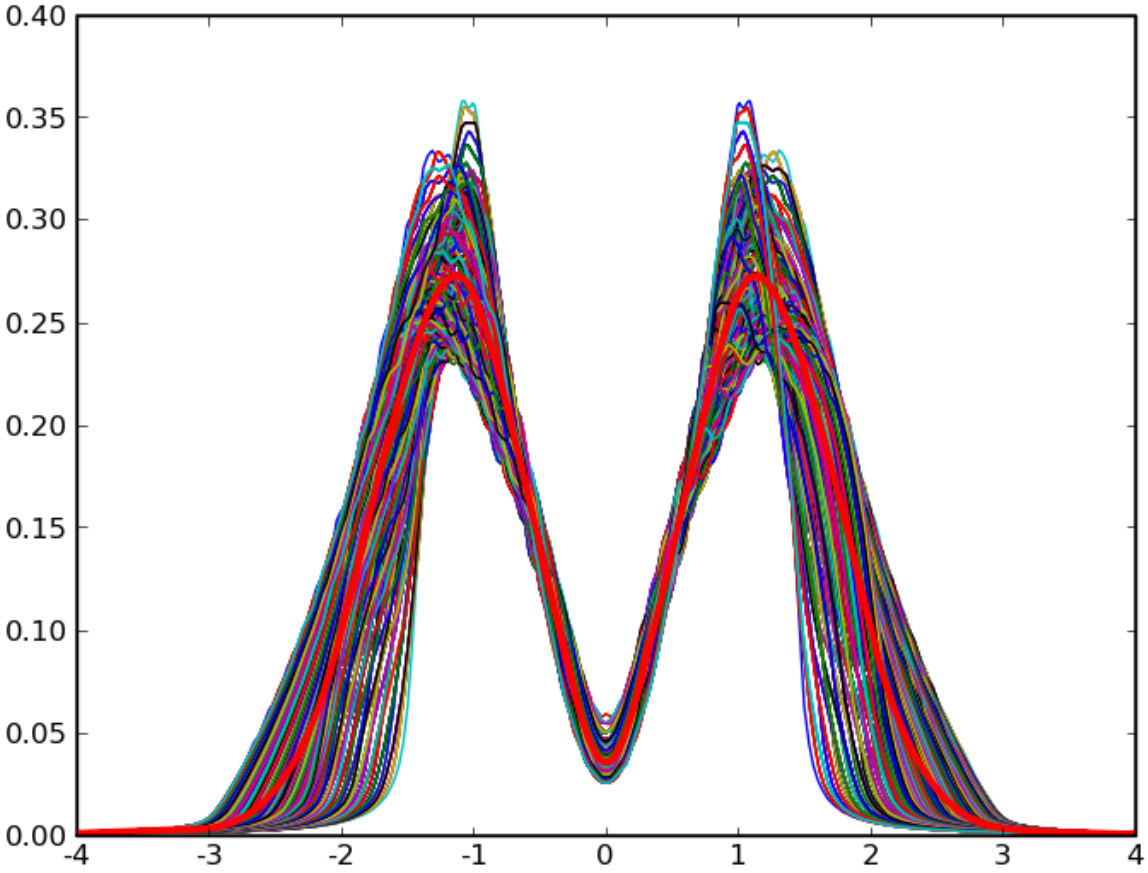

Figure 1: Self-energy at $U/(4t) = 1$ for all momentum points. Its momentum dependence is not very strong. The local self-energy (average over momentum) is displayed by red tick line.

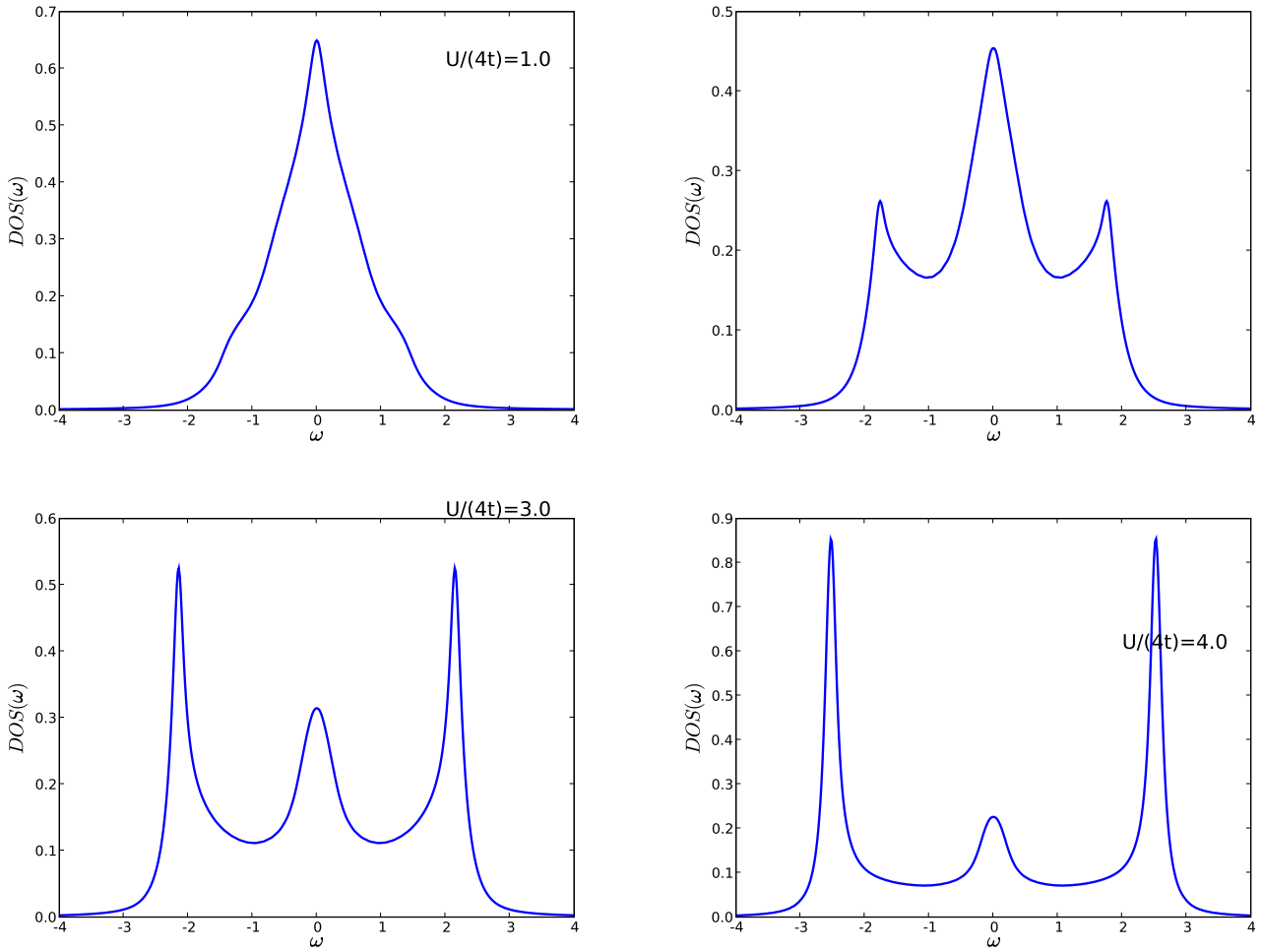

Figure 2: Density of states for the Hubbard model in 2D in the second order perturbation theory. Frequency is in units of $4t$. U is increasing $U/(4t) = 1, 2, 3, 4$. No Mott transition is observed. We used 24×24 k-points and 501 frequency points, $T = 0.03$, and broadening $\delta = 0.06$.

For 2D square lattice the self-energy has substantial momentum dependence as compared to the 3D case. Here connectivity is $z = 4$

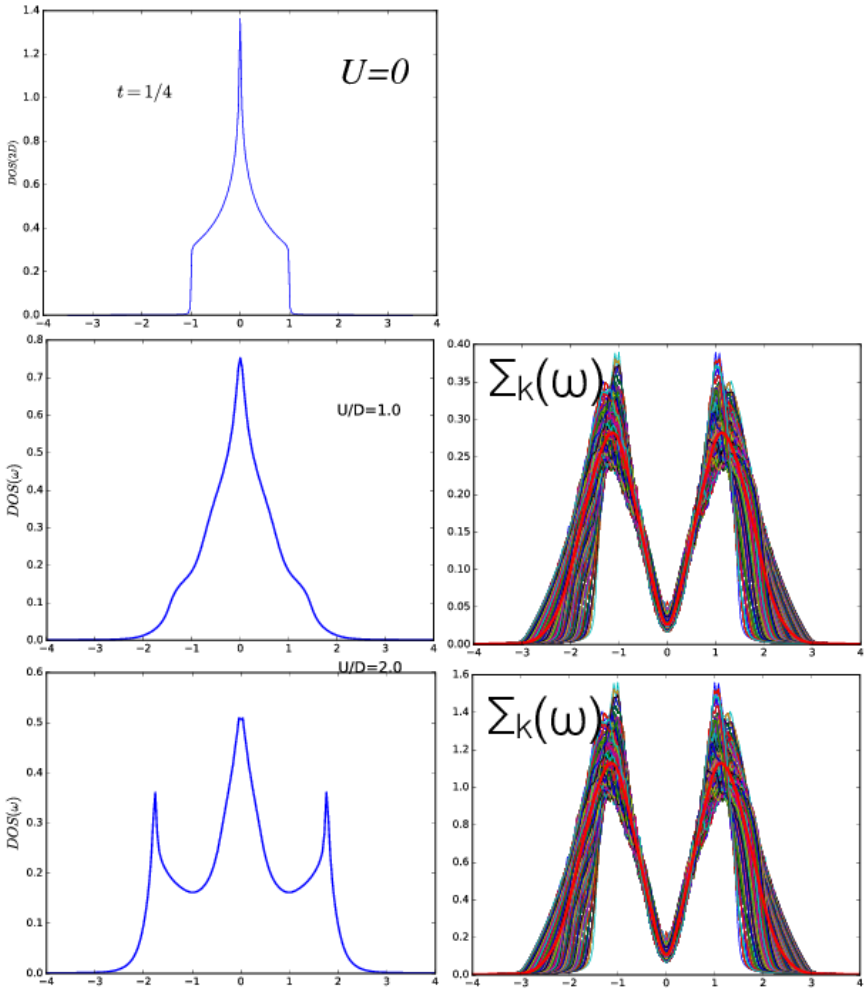

For fcc lattice the connectivity is $z = 12$ and momentum dependence of the self-energy is extremely weak.

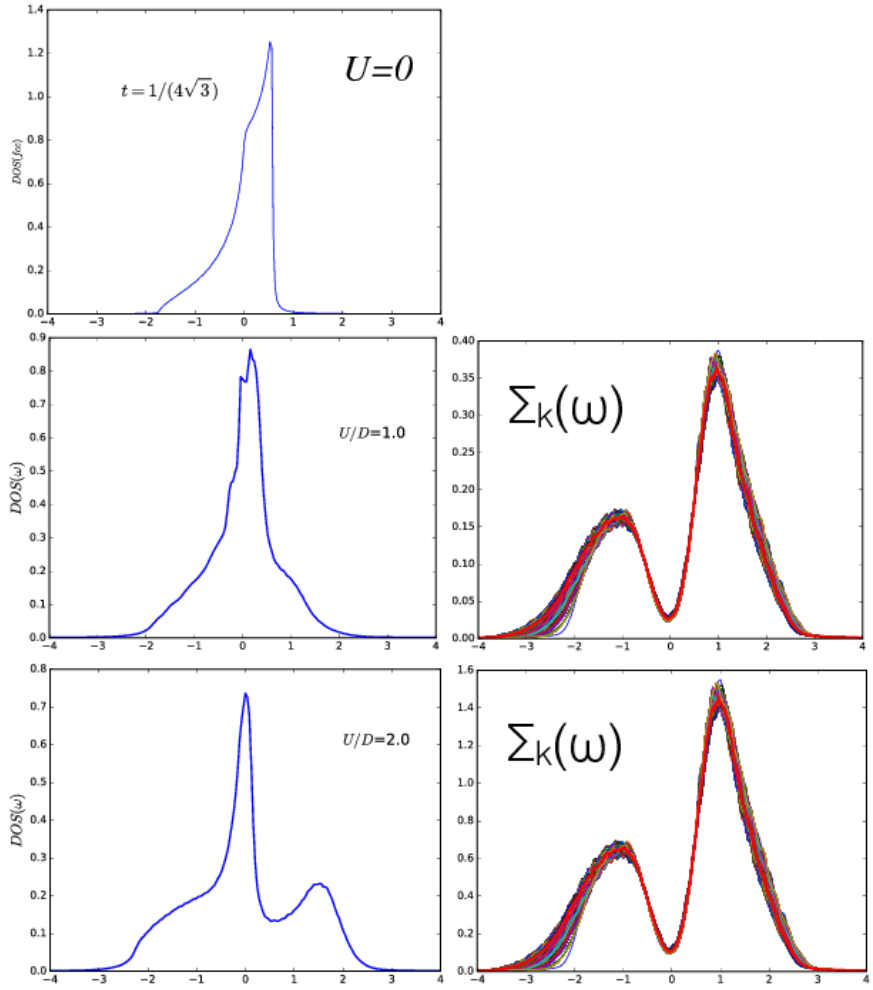

2 Local Approximation

As is clear from the Fig. 1 the self-energy does not varry very much from one momentum point to another. Hence, we would like to approximate the self-energy with momentum independent ansatz, i.e., $\Sigma_{\mathbf{k}}(\omega) \approx \Sigma_{loc}(\omega)$. In order to have purely local self-energy, we need to replace the momentum dependent propagator $G_{\mathbf{k}}$ in the Feynman diagrams with the purely local counterpart G_{loc}. The advantage of this method is that we can then go beyond the lowest order approximation. We will show in the later sections that the local self-energy Σ_{loc} can be computed by an appropriate auxiliary impurity problem. If we can solve the impurity problem exactly, we have the exact local self-energy. This approximation is called Dynamical Mean Field Theory, and becomes exact in the limit of large coordination number (large dimensions).

The Green's function of the "best" impurity problem (which delivers the "best" local self-energy) is the same as the local Green's function, i.e., $G_{imp} = G_{loc}$. The self-energy of the impurity is the local self-energy of the lattice problem, i.e., $\Sigma_{imp} = \Sigma_{loc}$. This constitutes the so called *"Dynamical Mean Field Theory"* (DMFT) equations. The DMFT

self-consistency condition is thus

$$\sum_{\mathbf{k}} \frac{1}{\omega - \epsilon_{\mathbf{k}} - \Sigma_{imp}} = G_{imp} \equiv \frac{1}{G^0_{imp}(\omega)^{-1} - \Sigma_{imp}} \tag{27}$$

hence, if we have an approximation for the impurity self-energy (impurity solver), we can compute the impurity propagator

$$G^0_{imp} = \left(\left(\sum_{\mathbf{k}} \frac{1}{\omega - \epsilon_{\mathbf{k}} - \Sigma_{imp}} \right)^{-1} + \Sigma_{imp} \right)^{-1} \tag{28}$$

which can be used by the impurity solver to obtain the impurity self-energy. Once the impurity self-energy is known, we can recompute G^0_{imp}. We have to repeat the procedure until self-consistency.

Hence in the final solution, the impurity green's function G_{imp} and the impurity self-energy Σ_{imp} are equal to their local counterparts, G_{loc} and Σ_{loc}.

Currently, the most precise "impurity solvers" are quantum Monte Carlo methods. But in this chapter, we will use the second order perturbation theory for the impurity solver. In this context, the second order solver was named the Iterative Perturbation Theory (IPT).

The second order self-energy has the same form as in Eqs. (8) and (9), except that the momentum index is replaced by the impurity propagator $G_{\mathbf{k}} \to G^0_{imp}$. Since the impurity propagator does not have the simple pole form, we need to work out the equations in terms of arbitrary G^0 function.

We will compute the imaginary part of the self-energy directly, and later we will recompute the real part by the Kramars-Kronig relation (which is valid for any analytic causal quantity), i.e.

$$\Sigma'(\omega) = -\frac{1}{\pi}\int \frac{\Sigma''(x)}{\omega - x} \tag{29}$$

We take the imaginary part of Eqs. (8) and 9, and replace the momentum dependent propagator with its local counterpart to obtain

$$P''(\Omega) = \int \frac{dx}{\pi} G^{0\prime\prime}(x) G^{0\prime\prime}(x-\Omega)\left[f(x) - f(x-\Omega)\right] \tag{30}$$

$$\Sigma''(\omega) = -U^2 \int \frac{dx}{\pi}[n(x) + f(x-\omega)]P''(x)G^{0\prime\prime}(\omega - x) \tag{31}$$

It is easy to show that

$$f(x) - f(x-\Omega) = \frac{f(-x)f(x-\Omega)}{n(-\Omega)} = -\frac{f(x)f(\Omega-x)}{n(\Omega)}$$

and

$$n(x) + f(x-\omega) = n(x)f(\omega-x) - f(x-\omega)n(-x)$$

If we define the following polarizations

$$P^{(1)}(\omega) = \int \frac{dx}{\pi} f(-x)f(x-\Omega)G^{0\prime\prime}(x)G^{0\prime\prime}(x-\Omega) \quad (32)$$

$$P^{(2)}(\omega) = \int \frac{dx}{\pi} f(x)f(\Omega-x)G^{0\prime\prime}(x)G^{0\prime\prime}(x-\Omega) \quad (33)$$

we can rewrite

$$\Sigma''(\omega) = U^2 \int \frac{dx}{\pi} \left[f(\omega-x)P^{(2)}(x) + f(x-\omega)P^{(1)}(x) \right] G^{0\prime\prime}(\omega-x) \quad (34)$$

We will express both polarization and the self energy in terms of the following modified spectral functions

$$A^+(\omega) = -\frac{1}{\pi}G^{0\prime\prime}(x)f(x) \quad (35)$$

$$A^-(\omega) = -\frac{1}{\pi}G^{0\prime\prime}(x)f(-x) \quad (36)$$

We finally obtain

$$P^{(1)}(\omega) = \pi \int dx A^-(x)A^+(x-\Omega) \quad (37)$$

$$P^{(2)}(\omega) = \pi \int dx A^+(x)A^-(x-\Omega) \quad (38)$$

and

$$\Sigma''(\omega) = -U^2 \int dx [A^+(\omega - x)P^{(2)}(x) + A^-(\omega - x)P^{(1)}(x)] \quad (39)$$

2.1 The algorithm

1 create equidistant mesh of frequency points

2 define the fermi function on this mesh $f(\omega)$

3 create the index array for frequency difference $\omega - \Omega$.

4 prepare the non-interacting density of states $D(\omega)$. It is easier to converge the solution for semicircular density of states $\frac{\sqrt{(4t)^2-x^2}}{2\pi(2t)^2}$, although 2D has very similar solution. We will choose the unit of energy $4t = 1$, so that $D(x) = 2/\pi\sqrt{1-x^2}$

5 Code the Hilbert transform

$$w(z) = \int d\omega \frac{D(\omega)}{z-\omega}$$

which should work for any complex z. For semicircular DOS we can compute the Hilbert transform analytically, and it takes the form:

$$w(z) = 2(z - \text{sign}(Rez)\sqrt{z^2-1}) \tag{40}$$

6 Compute A^+ and A^- defined in Eqs. 35 and 36.

7 Compute the polarization Eq. 37 and 38.

8 Compute $\Sigma(\omega)$ of Eq. 39.

9 Compute the Green's function using the Hilbert transform $G(\omega) = w(\omega - \Sigma(\omega))$.

10 Recompute G^0 by the equation: $G^0 = 1/(1/G + \Sigma)$, derived in Eq.28.

11 Go back to step 6 and recomputing A^+ and A^- again using new G^0.

Do not get discouraged if the convergence is not very good. Close to the Mott transition, the convergence is very hard to achieve. One needs to mix the solution very slowly.

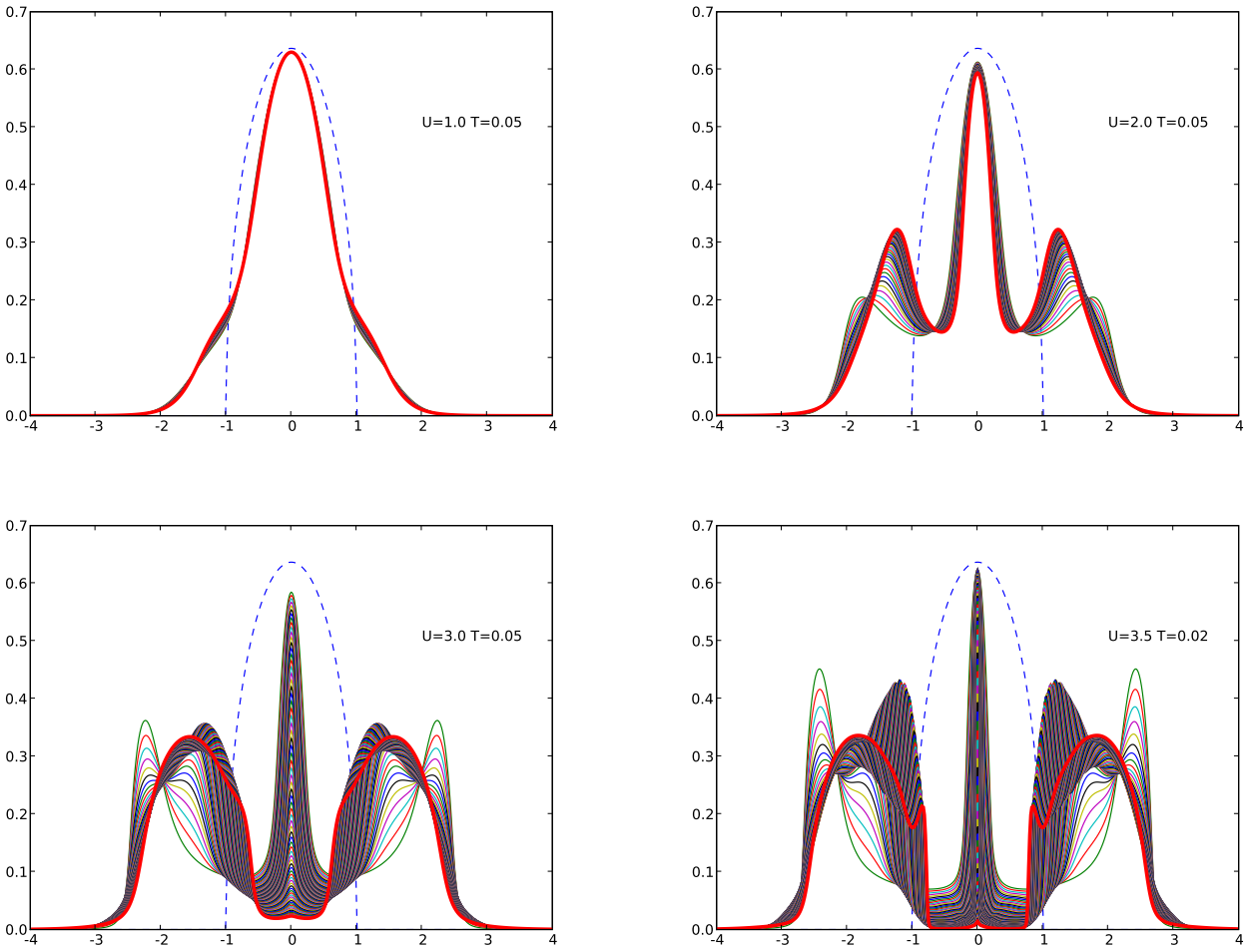

Figure 3: Density of states for the Hubbard model for the Bethe lattice for $U = 1, 2, 3, 3.5$. The system is bad metal at $U = 3.0$ and becomes good metal at lower temperature. It is an insulator at $U = 3.5$. The solution is shown in bold red. All iterations are plotted.

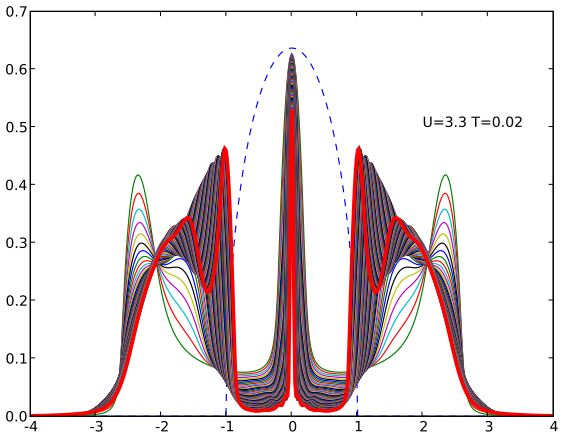

Figure 4: Although the system is almost insulating at finite temperature, it becomes a good metal at lower temperature; it becomes coherent.

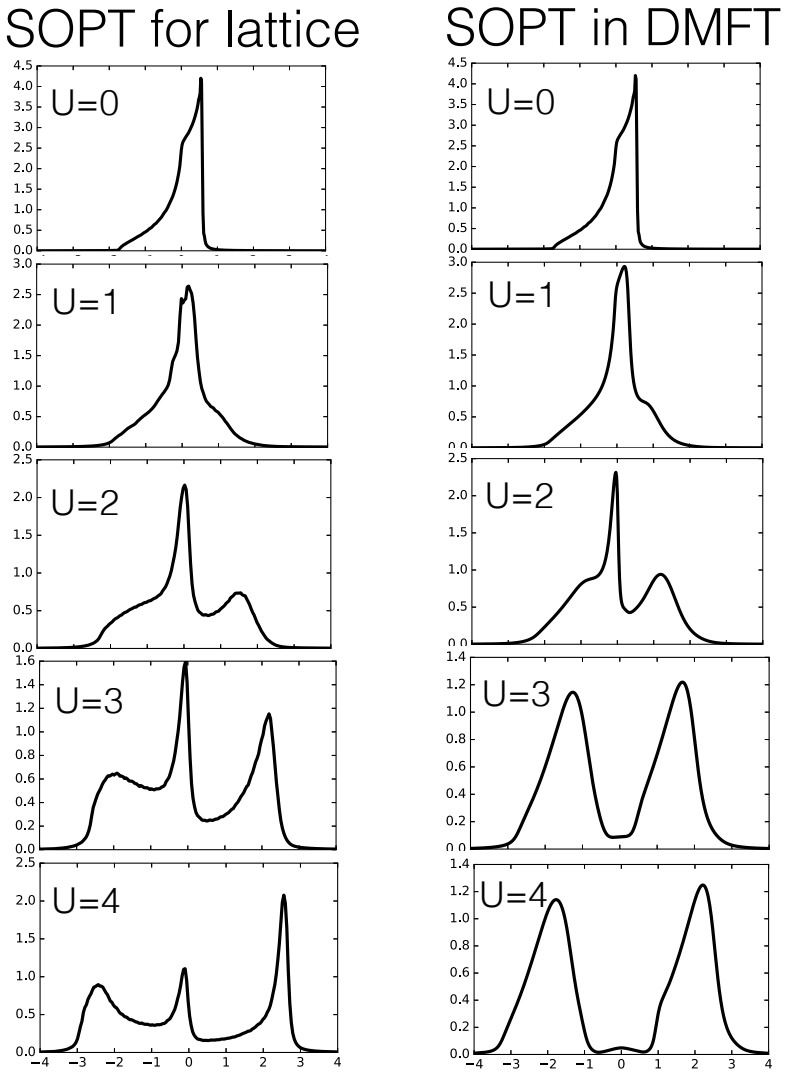

Figure 5: Comparison between direct second order perturbation on the fcc lattice, and the local second-order approximation (using DMFT SCC) on the fcc lattice.